

Electronic Transitions at the CaF₂/Si(111) Interface Probed by Resonant Three-Wave-Mixing Spectroscopy

T. F. Heinz, F. J. Himpsel, and E. Palange^(a)

IBM Research Division, T. J. Watson Research Center, Yorktown Heights, New York 10598

E. Burstein

Department of Physics, University of Pennsylvania, Philadelphia, Pennsylvania 19104

(Received 3 February 1989)

Resonant optical second-harmonic and sum-frequency generation are applied to probe electronic transitions at the Ca-terminated epitaxial CaF₂/Si(111) interface. A band gap of 2.4 eV is established for the interface states, a value twice as large as that in bulk Si, but only $\frac{1}{5}$ of the band gap in CaF₂. The experimental three-wave-mixing spectra can be modeled by a two-dimensional band gap and a narrow resonance 150 meV below the band edge, the latter being tentatively assigned to a transition to a bound two-dimensional exciton.

PACS numbers: 73.20.-r, 42.65.Ma, 78.65.-s

Understanding the nature of solid/solid interfaces is an area of great fundamental and practical importance. The characteristics of interfaces strongly influence the behavior of electronic devices with small dimensions and are critical in determining the morphology of thin-film growth, particularly in the case of epitaxial structures. Fully developed buried interfaces present difficulties for analysis: The unique features of the interface are present only in a few atomic layers of material, but the interfacial region will generally be covered by an overlayer of many times this thickness. Consequently, many of the sensitive and highly developed techniques appropriate for surfaces may not be suitable for this interesting class of problems. In this Letter, we present the first application of three-wave-mixing spectroscopy to the problem of solid/solid interfaces. The method is purely optical and can, because of its large probing depth, be used to investigate buried interfaces. It relies on the second-order nonlinear optical processes of second-harmonic and sum-frequency generation. These effects are forbidden (within the electric-dipole approximation) in centrosymmetric media and, hence, exhibit a high degree of sensitivity to interfaces, where the inversion symmetry must be broken.¹ The technique has been previously employed in studies of the electronic^{2,3} and vibrational^{4,5} spectra of molecular monolayers. Here we report for three-wave-mixing spectroscopy of the epitaxial interface of CaF₂/Si(111). This material system⁶⁻¹² has recently attracted considerable attention as a prototype of a well-controlled semiconductor/insulator interface, as well as for its potential technological importance. The resonant second-harmonic and sum-frequency spectra presented in this work permit a value for the previously unknown interface band gap to be established directly. The observed energy difference of 2.4 eV between the filled and empty interface states stands in marked contrast to the band gaps of the bulk Si (1.1 eV) and CaF₂ (12.1 eV), indicating the distinctive nature of the interfacial region.

The three-wave-mixing spectra for the CaF₂/Si(111) interface were obtained by exposing the sample to laser radiation from a tunable source. The intensity of the reflected light at the second-harmonic (SH) frequency was measured as a function of wavelength. Sum-frequency (SF) data were collected for mixing of the tunable source with the light from a laser operating at a fixed frequency. Tunable radiation consisting of 5-nsec pulses was produced by a dye laser pumped by the frequency-doubled or -tripled output of a Q-switched Nd-doped yttrium aluminum garnet (Nd:YAlG) laser. With a weakly focused pump beam (diam > 1 mm), we obtained an easily measurable three-wave-mixing (SH or SF) signal from the sample with a laser fluence (~1 mJ) far below the damage threshold. The SH or SF light was detected by a photomultiplier and gated electronics after being isolated by appropriate spectral filtering. To compensate for changes in the characteristics of the pump radiation and the detection system as the dye laser was scanned, the signal was simultaneously recorded from a parallel optical path in which the three-wave-mixing process occurred in a quartz plate. The CaF₂/Si(111) samples consisted of a layer of ~500 Å of CaF₂ grown epitaxially on a Si(111) crystal face, following a procedure described previously.^{10,11} Since the Fermi level is found to be pinned by the CaF₂/Si(111) interface near the valence-band maximum of Si,¹⁰ a lightly p-doped Si substrate was chosen to eliminate any possible band bending in our samples. In general, both Ca and F atoms may form bonds with Si atoms at the interface. Here we investigate Ca-terminated interfaces formed by subjecting the samples to a rapid heating cycle after deposition of the CaF₂ film.⁷

The material response in a three-wave-mixing experiment can be characterized (in the electric-dipole approximation) by a quadratic susceptibility relating the nonlinear source polarization to the pump electric fields:

$$\mathbf{P}^{\text{NLS}}(\omega_3) = \chi^{(2)}(\omega_3 = \omega_1 + \omega_2) : \mathbf{E}(\omega_1)\mathbf{E}(\omega_2),$$

with ω_3 being the frequency of the radiation produced by sum-frequency generation (SFG) from pump electric fields with frequencies ω_1 and ω_2 . In the bulk of centrosymmetric media, one can readily see from parity considerations that $\chi^{(2)}$ must vanish; the relation is, however, applicable for an asymmetric interfacial region. At an interface, it is convenient to consider an induced nonlinear dipole moment per unit area (rather than per unit volume) and the corresponding surface nonlinear susceptibility tensor ${}^s\chi^{(2)}$. The surface nonlinear susceptibility (together with the linear optical properties of the media) determines the polarization and frequency dependence of three-wave-mixing signals. For the second-harmonic generation (SHG) process with a pump frequency ω , we can write the intensity (in cgs units) of the beam reflected into a medium with dielectric constant ϵ as¹³

$$I(2\omega) = 32\pi^3 c^{-3} \omega^2 \epsilon^{-1}(\omega) \epsilon^{-1/2}(2\omega) \sec^2 \theta |\mathbf{e}(2\omega) \cdot {}^s\chi^{(2)} : \mathbf{e}(\omega) \mathbf{e}(\omega)|^2 I^2(\omega). \quad (1)$$

Here θ denotes the angle of the radiated SH beam with respect to the surface normal, the symbols $\mathbf{e}(\omega)$ and $\mathbf{e}(2\omega)$ refer, respectively, to the polarization vectors of the fundamental and harmonic fields after correction by the Fresnel factors appropriate for wave propagation to the interface, and $I(\omega)$ represents the intensity of the incident pump radiation at the fundamental frequency.

The tensor properties of the nonlinear susceptibility reflect the structure of the interface and, hence, permit one to assess the symmetry and order present at the interface. To describe the nonlinear susceptibility tensor, we introduce a coordinate system with \hat{x} and \hat{y} in the plane of the interface, aligned, respectively, along the $[2\bar{1}\bar{1}]$ and $[01\bar{1}]$ axes of the Si crystal, and $\hat{z} \parallel [111]$. The bulk Si structure will then exhibit a threefold symmetry for rotations about the z axis and mirror symmetry with respect to the x - z plane. If this $3m$ symmetry is also present at the $\text{CaF}_2/\text{Si}(111)$ interface, we can enumerate the independent tensor elements of ${}^s\chi^{(2)}$. For both SHG and SFG, there is a single independent tensor element associated with an anisotropic response, i.e., a response that varies with rotation of the sample about the surface normal: ${}^s\chi_{xxx}^{(2)} = -{}^s\chi_{xxy}^{(2)} = -{}^s\chi_{xyx}^{(2)} = -{}^s\chi_{yyy}^{(2)}$. The nonlinear susceptibility for SHG also has three independent isotropic tensor elements: ${}^s\chi_{zzz}^{(2)}$, ${}^s\chi_{zxx}^{(2)} = {}^s\chi_{zyy}^{(2)}$, and ${}^s\chi_{xzx}^{(2)} = {}^s\chi_{xxz}^{(2)} = {}^s\chi_{yzy}^{(2)} = {}^s\chi_{yyz}^{(2)}$. The more general process of SFG gives rise to an additional independent isotropic element, since ${}^s\chi_{xzx}^{(2)} = {}^s\chi_{yzy}^{(2)} \neq {}^s\chi_{xxz}^{(2)} = {}^s\chi_{yyz}^{(2)}$.

The symmetry properties of the $\text{CaF}_2/\text{Si}(111)$ interface were probed by recording the SH intensity as the sample was rotated about its surface normal. We have examined the behavior for parallel polarizations of the pump and SH radiation with excitation at normal incidence. Within experimental accuracy, the variation in the SH intensity as function of sample orientation can be described by the relation $I_\phi(2\omega) \sim \cos^2 3\phi$, where ϕ denotes the angle between the pump polarization vector and the $[2\bar{1}\bar{1}]$ direction in the surface. This expression agrees with the predictions of Eq. (1) for ${}^s\chi^{(2)}$ with $3m$ symmetry.¹⁴ Our finding of $3m$ symmetry interface is in accord with recent microscopic structural models of the $\text{CaF}_2/\text{Si}(111)$ interface.⁸

The resonant three-wave-mixing spectra give information about the spacing of electronic transitions occurring at the interface. Each independent tensor element of ${}^s\chi^{(2)}$ will, in general, manifest different resonances, since

the selection rules apply. In this work, we have examined the nonlinear response arising from ${}^s\chi_{zzz}^{(2)}$, which includes (in the dipole approximation) contributions from transitions with moments perpendicular to the interface. In the experimental measurements, we detected the p -polarized three-wave-mixing radiation produced by excitation with a p -polarized beam incident on the sample at 80° from the surface normal. For this configuration, ${}^s\chi_{zzz}^{(2)}$ is accessed together with other tensor elements. Examination of the polarization dependence of the SHG process revealed, however, that the contribution of ${}^s\chi_{zzz}^{(2)}$ dominated the observed signal.¹⁵

Figure 1(a) displays the resonant SH spectrum associated with ${}^s\chi_{zzz}^{(2)}$ for the $\text{CaF}_2/\text{Si}(111)$ interface. Measurements have also been performed for somewhat lower

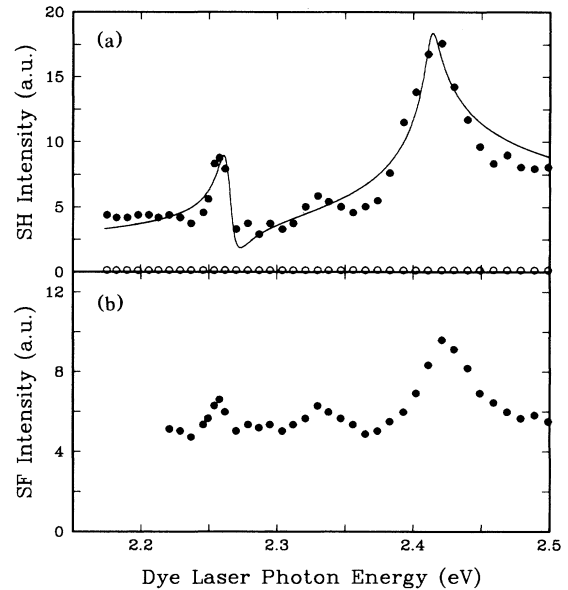


FIG. 1. Resonant three-wave-mixing signals associated with ${}^s\chi_{zzz}^{(2)}$ as a function of the energy of a photon from the tunable dye laser. (a) Results for the SHG process and (b) the case of SFG involving mixing the output of the dye laser with a photon of fixed energy (1.17 eV). The filled symbols refer to signals from the $\text{CaF}_2/\text{Si}(111)$ sample; the open symbols to a $\text{Si}(111)$ surface covered by the native oxide. The solid curve in (a) is a fit to theory, as discussed in the text.

photon energies than shown, but no additional structure was observed. Before discussing the detailed interpretation of the spectrum, we need to justify our implicit assumption that the nonlinear response can be attributed entirely to the $\text{CaF}_2/\text{Si}(111)$ interface. There are, in fact, two other possible contributions to the nonlinear radiation: the surface of the CaF_2 (away from the Si) and the higher-order (electric quadrupole and magnetic dipole) terms in the bulk media.¹³ A direct comparison has been made with a Si(111) sample covered by the native oxide. As can be seen in Fig. 1(a), the signal strength from this sample over the given range of energies is negligible compared with the sample of interest. This result demonstrates that the bulk nonlinearity of the Si can be neglected. The contribution of upper surface and the bulk of the CaF_2 was found to be much smaller still in a measurement of SHG from the surface of a CaF_2 crystal.

To understand the information available from a resonant SH spectrum, let us recall that the SHG process can be described as a parametric conversion (three-wave mixing) of two photons at the pump frequency into a single photon at the SH frequency. This nonlinear conversion displays an enhancement when either the energy of a pump or SH photon coincides with that of a transition in the medium. Consequently, it is not immediately apparent whether the resonances observed in the resonant SH spectrum of Fig. 1(a) correspond to transitions at the fundamental or the SH photon energy. To eliminate this potential ambiguity, we have performed additional sum-frequency measurements. In Fig. 1(b), a spectrum is shown for the intensity of the SF radiation produced by mixing the radiation of the Nd:YAIG laser having a fixed photon energy of 1.17 eV with the variable frequency output of the dye laser. The SH and SF spectra (Fig. 1) exhibit the same resonant features, thus demonstrating that the resonances arise from transitions at the fundamental frequency of the dye laser.

Having now established that the resonances in the spectrum of Fig. 1 arise from transitions at the $\text{CaF}_2/\text{Si}(111)$ interface at the fundamental frequency, we turn to the interpretation of the features. We associate the strong peak at approximately 2.4 eV with the transitions at the interface band gap. This assignment is supported by the following reasoning. In a localized picture,¹⁰ we consider the interface states as arising from perturbed $\text{Ca}^+(4s)$ and $\text{Si}(3p)$ dangling-bond orbitals (Fig. 2). Such a description has emerged from a theoretical study of the isoelectronic Na/Si(111) system by Northrup.¹⁶ Neglecting the interaction between these orbitals, we would expect them to lie at the Fermi level, since they are half filled. When the orbitals hybridize to form a bonding combination, their energy is apparently reduced by ~ 1 eV, as indicated by the position of the interface valence band in photoemission spectra.¹¹ One then anticipates that the corresponding antibonding

states will be positioned roughly 1 eV above the Fermi level, producing a semiconducting interface with an energy separation on the order of 2 eV between the valence and conduction bands. Our experimental results yield an interface band gap of 2.4 eV.

We now discuss the shape of the main feature in the resonant SH spectrum at 2.4 eV and demonstrate that it is compatible with a direct band gap in two dimensions. From Eq. (1), we note that the resonant SHG spectrum is proportional to $|\chi_{zzz}^{(2)}|^2$. Thus the spectrum cannot be interpreted solely in terms of $\text{Im}[\chi^{(2)}]$, which is associated with the oscillator strength of transitions at each energy, but must also include the dispersive contribution from $\text{Re}[\chi^{(2)}]$. The expected line shape can, nonetheless, be related to the resonant absorption profile ($\text{Im}[\chi^{(2)}]$) by means of a Kramers-Kronig analysis. To model a direct transition between two-dimensional bands, we assume that near the band edge $\text{Im}[\chi_{zzz}^{(2)}(2\omega = \omega + \omega)] \propto J_{\text{DOS}}(\hbar\omega)$, with $J_{\text{DOS}}(\hbar\omega)$ representing the joint density of states for transitions between the valence and conduction bands with energy $\hbar\omega$. For a direct band gap in two dimensions, $J_{\text{DOS}}(\hbar\omega) \propto (\hbar\omega - \hbar\omega_g)$. Here θ is a step function and $\hbar\omega_g$ is the energy of the band gap. In order to obtain physically meaningful results, we must include a finite cutoff energy $\hbar\omega_c$ for the J_{DOS} and allow for a nonzero linewidth Γ of the transitions. The solid curve in Fig. 1(a) resulting from this simple analysis (with $\hbar\omega_g = 2.41$ eV, $\hbar\omega_c \approx 5$ eV, and $\Gamma = 9$ meV FWHM) reproduces the experimental line shape of the band edge reasonably well.

The treatment of resonant three-wave-mixing spectra in the vicinity of a two-dimensional interband transition

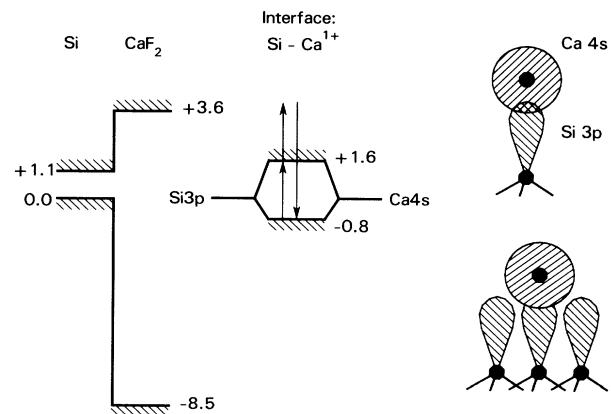


FIG. 2. Band-gap structure of the $\text{CaF}_2/\text{Si}(111)$ interface. The offsets of the bulk bands and the location of the occupied interface state are taken from Refs. 10 and 11, respectively. The position of the unoccupied interface state has been determined in this work. The right column is a schematic representation of hybridized $\text{Si}(3p)$ dangling-bond and $\text{Ca}^+(4s)$ orbitals at the interface for Ca atoms at high-symmetry (top and hollow) sites.

in the preceding paragraph did not make any allowance for excitonic effects, i.e., for the correlated motion of the electrons and holes. In two-dimensional systems these effects are particularly significant, as has been dramatically demonstrated in semiconductor quantum-well structures.¹⁷ We consider here excitons formed by delocalized carriers in the interface bands, the two-dimensional analog of Wannier excitons.¹⁸ Above the band edge, the excitonic enhancement leads only to a very gradual modulation in the transition strength over the relevant range of energies.¹⁸ Below the band edge, on the other hand, the existence of bound excitons should influence the spectra. In two dimensions, the binding energy of these excitons is increased with respect to three dimensions, since the familiar $1/n^2$ dependence in the Rydberg series of levels is replaced by $1/(n - \frac{1}{2})^2$:

$$E_n = -\mu e^4 / [\hbar^2 \epsilon^2 (n - \frac{1}{2})^2], \quad n=1,2,3,\dots \quad (2)$$

In this relation,¹⁸ the binding energies are measured with respect to the band edge, $\mu = (m_v^{-1} + m_c^{-1})^{-1}$ is given by the expected combination of the two-dimensional effective masses of the valence and conduction interface bands, and ϵ accounts for the dielectric screening of the Coulomb interaction between the two-dimensional carriers. Since the appropriate parameters are not well known for this problem, it is difficult to predict the positions of the excitonic levels. We tentatively assign the sharp feature appearing at 2.26 eV to the $n=1$ exciton. From the measured interface valence-band dispersion and estimated conduction-band dispersion in Ref. 11, we obtain $\mu \sim 0.6m_0$ for the reduced mass, where m_0 represents the mass of a free electron. The observed excitonic binding energy¹⁹ of 150 meV is then reproduced by Eq. (2) for $\epsilon=15$. This value, comparable to the low-frequency dielectric constant of Si, may be representative of the dielectric properties of the interfacial region formed by the Si-Ca bonds.

The solid curve in Fig. 1(a) includes the influence of a bound excitonic state. This was accomplished by adding a Lorentzian contribution to $\text{Im}[^s\chi_{zzz}^{(2)}]$ centered at 2.26 eV with a width of 11 meV (FWHM). In both the SH and SF spectra, a feature can also be seen at an energy of ~ 2.33 eV. While it is tempting to associate the resonance with an $n=2$ exciton, Eq. (2) shows that this level should lie at considerably higher energy. In fact, additional experimental studies indicate that the feature is attributable to the presence of a small contribution of $^s\chi_{zzx}^{(2)}$ to the measured three-wave-mixing signal. Since the occupied interface state has Δ_1 symmetry (like an s or p_z orbital) near the zone center,¹¹ $^s\chi_{zzz}^{(2)}$ will exhibit resonances (in the dipole approximation) only for transition to states of Λ_1 symmetry. On the other hand, the $^s\chi_{zzx}^{(2)}$ tensor element includes contributions from states of

Λ_3 symmetry (p_x, p_y character), which may account for the additional feature at ~ 2.33 eV. A more complete discussion of the features of the three-wave-mixing spectra associated with different tensor elements of $^s\chi^{(2)}$ and a model for the nonlinear response of the interface based on hybridized bonding and antibonding orbitals will be presented elsewhere.¹⁵

^(a)On leave from the University of Rome, Rome, Italy.

¹Y. R. Shen, *Annu. Rev. Mater. Sci.* **16**, 69 (1986); G. I. Richmond, J. M. Robinson, and V. L. Shannon, *Prog. Sur. Sci.* **28**, 1 (1988).

²T. F. Heinz, C. K. Chen, D. Ricard, and Y. R. Shen, *Phys. Rev. Lett.* **48**, 478 (1982).

³N. E. Van Wyck, E. W. Koenig, J. D. Byers, and W. M. Hetherington, III, *Chem. Phys. Lett.* **122**, 153 (1985).

⁴X. D. Zhu, H. Suhr, and Y. R. Shen, *Phys. Rev. B* **35**, 3047 (1987); J. H. Hunt, P. Guyot-Sionnest, and Y. R. Shen, *Chem. Phys. Lett.* **133**, 189 (1987); P. Guyot-Sionnest, J. H. Hunt, and Y. R. Shen, *Phys. Rev. Lett.* **59**, 1597 (1987).

⁵A. L. Harris, C. E. D. Chidsey, N. J. Levinos, and D. N. Loiacono, *Chem. Phys. Lett.* **141**, 350 (1987).

⁶L. J. Schowalter and R. W. Fathauer, *J. Vac. Sci. Technol. A* **4**, 1026 (1986), and references therein.

⁷F. J. Himpfel, U. O. Karlsson, J. F. Morar, D. Rieger, and J. A. Yarmoff, *Mater. Res. Soc. Symp. Proc.* **94**, 181 (1987), and references therein.

⁸R. M. Tromp and M. C. Reuter, *Phys. Rev. Lett.* **61**, 1756 (1988), and references therein.

⁹M. A. Olmstead, R. I. G. Uhrberg, R. D. Bringans, and R. Z. Bachrach, *Phys. Rev. B* **35**, 7526 (1987).

¹⁰F. J. Himpfel, U. O. Karlsson, J. F. Morar, D. Rieger, and J. A. Yarmoff, *Phys. Rev. Lett.* **56**, 1497 (1986); D. Rieger, F. J. Himpfel, U. O. Karlsson, F. R. McFeely, J. F. Morar, and J. A. Yarmoff, *Phys. Rev. B* **34**, 7295 (1986).

¹¹A. B. McLean and F. J. Himpfel, *Phys. Rev. B* **39**, 1457 (1989).

¹²K. Nath and A. B. Anderson, *Phys. Rev. B* **38**, 8264 (1988); S. Satpathy and R. M. Martin, *Phys. Rev. B* **39**, 8494 (1989).

¹³Y. R. Shen, *The Principles of Nonlinear Optics* (Wiley, New York, 1984), Chap. 25.

¹⁴T. F. Heinz, M. M. T. Loy, and W. A. Thompson, *Phys. Rev. Lett.* **54**, 63 (1985); *J. Vac. Sci. Technol. B* **3**, 1467 (1985).

¹⁵T. F. Heinz, F. J. Himpfel, E. Palange, and E. Burstein (to be published).

¹⁶J. E. Northrup, *J. Vac. Sci. A* **4**, 1404 (1986).

¹⁷D. S. Chemla, *Scr. Phys. Acta* **56**, 607 (1983).

¹⁸M. Shinada and S. Sugano, *J. Phys. Soc. Jpn.* **21**, 1936 (1966).

¹⁹The effective Rydberg for the interface exciton is $\frac{1}{4}$ of the binding energy, viz., 38 meV. By comparison, the effective Rydberg for bulk Si is 14 meV [K. L. Shaklee and R. E. Nahory, *Phys. Rev. Lett.* **24**, 942 (1970)].